World Academy of Science, Engineering and Technology
International Journal of Aerospace and Mechanical Engineering
Vol:18, No:10, 2024

Stability Analysis and Controller Design of Further Development of MIMOS II for Space Applications with Focus on the Extended Lyapunov Method: Part I

Mohammad Beyki, Justus Pawlak, Robert Patzke, Franz Renz

Abstract—In the context of planetary exploration, the MIMOS II (miniaturized Mössbauer spectrometer) serves as a proven and reliable measuring instrument. The transmission behaviour of the electronics in the Mössbauer spectroscopy is further developed and optimized. For this purpose, the overall electronics is split into three parts. This elaboration deals exclusively with the first part of the signal chain for the evaluation of photons in experiments with gamma radiation. Parallel to the analysis of the electronics, an additional method for analysing the stability of linear and non-linear systems is presented: The extended method of Lyapunov's stability criteria. The design helps to weigh advantages and disadvantages against other simulated circuits in order to optimize the MIMOS II for the terestric and extraterestric measurment. Finally, after stability analysis, the controller design according to Ackermann is performed, achieving the best possible optimization of the output variable through a skillful pole assignment.

Keywords—Controller design for MIMOS II, stability analysis, Mössbauer spectroscopy, electronic signal amplifier, light processing technology, photocurrent, transimpedance amplifier, extended Lyapunov method.

I. Introduction

MÖSSBAUER spectroscopy stands as a highly precise and invaluable analytical technique within the realm of solid-state physics and materials science. It facilitates the examination of atomic and nuclear properties of materials in a manner unrivaled by other methods. This methodology relies on the interaction of gamma rays with atomic nuclei within a solid. What sets Mössbauer spectroscopy apart is its unique capacity to provide detailed information about energy levels and structural characteristics at the atomic scale. This technique finds diverse applications, ranging from the investigation of crystal structures to the characterization of chemical bonding and magnetic properties in materials.

M. Beyki is with Department of Integrated Circuits and Embedded Systems, University of Applied Sciences and Arts Hannover, Germany; Institute of Inorganic Chemistry, Leibniz University Hannover, Germany and Laboratory of Nano and Quantum Engineering, Leibniz University Hannover, Germany (e-mail: mohammad.beyki@acd.uni-hannover.de).
J. Pawlak is with Institute of Inorganic Chemistry, Leibniz University Hannover, Germany and Laboratory of Nano and Quantum Engineering, Leibniz University Hannover, Germany (e-mail: justus.pawlak@acd.uni-hannover.de).
R. Patzke is with Department of Integrated Circuits and Embedded Systems, University of Applied Sciences and Arts Hannover, Germany (e-mail: robert.patzke@hs-hannover.de).
F. Renz is with Institute of Inorganic Chemistry, Leibniz University Hannover, Germany (e-mail: franz.renz@acd.uni-hannover.de).

A. Miniaturized Mössbauer Spectrometer

The MIMOS II (miniaturised Mössbauer spectrometer) has now been in use for over a decade in planetary exploration and has provided reliable and robust measurement data from unknown areas [1]. The MIMOS II originally devised by Göstar Klingelhöfer, is further developed by the Renz group at the Leibniz University Hanover in cooperation with the Hanover University of Applied Sciences [1], [2]. Fig. 1 illustrates the configuration of the Mössbauer spectrometer as a schematic diagram:

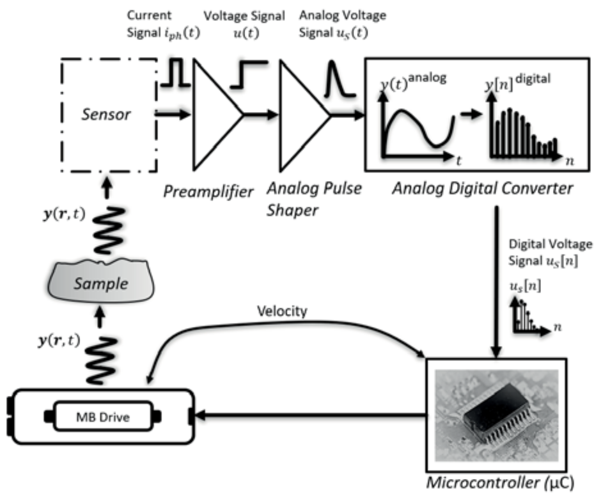

Fig. 1 Schematic representation of the Mössbauer spectrometer

The Mössbauer drive mechanically oscillates radioactive Co-57 sources to exploit the Doppler effect for the purpose of increasing the number of protons encountered by emitted gamma rays. The emitted gamma rays interact with the sample, elevating the energy level of activated protons. After a certain period, the protons return to their original energy state and emit gamma rays. These gamma rays are detected by a sensor and subsequent electronics for digitalization. A microcontroller further processes the acquisition data and concurrently controls the Mössbauer drive.

B. Electronics behind Mössbauer Spectroscopy

The electronics for gamma-ray detection are the central focus of this paper. Photons impinge on the surface of the photosensor, generating a photocurrent $i_{\text{ph}}(t)$. The challenge in harnessing the sensor signal lies in generating an appropriate signal shaping into a voltage that is stable enough for further processing. The generated photocurrent is very low in amplitude and must be amplified in a manner that avoids signal distortion due to noise and other sources of interference. For this reason, the foundation of the signal shaping is a transimpedance amplifier. The current $i_{\text{ph}}(t)$ is converted into a voltage $u_{\text{a}}(t)$ and made available for further processing.

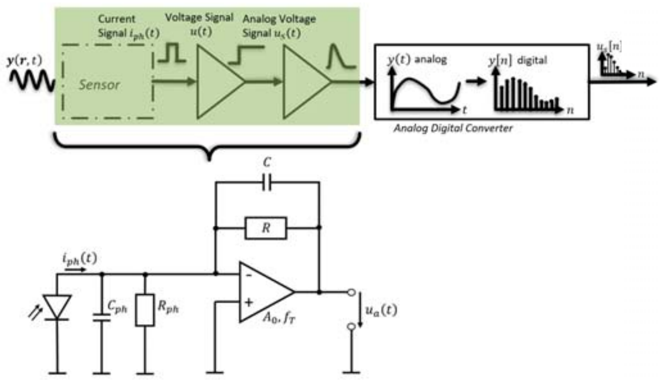

Fig. 2 Schematic representation of the electronics for the Mössbauer spectrometer

II. Introductory Consideration of the Transimpedance Amplifier

The transimpedance amplifier (TIA) is the core of the electrical circuit considered in this paper. In this elaboration, the already existing derivations for the mentioned system are used. Due to the fact that the measured and in the system theoretical analysis focused output voltage has an oscillatory characteristic, at least a second order system is assumed in the modeling of the TIA [3]-[5].

A. The TIA as a 2nd Order System

It has been proven that the TIA exhibits oscillations in certain operating ranges. With the modeling of the TIA as a second order system, output oscillations with limited quality can be approximately described. The cause of the oscillation is found in the modeling of the photodiode, which itself also has a capacitive and a resistive component [3], [4]. Fig. 3 shows such a second-order transimpedance amplifier.

Due to the fact that this paper mainly deals with the system analysis of the electrical circuits listed, the mathematical descriptions already known for a long time are used without further derivations. Derivation can be taken from corresponding literature [3]-[6].

Because of the inverting effect at the input of the operational amplifier, the output voltage is pushed into the negative range and only there shows oscillation characteristics (1).

$$G_{\text{PT2}}(s) = \frac{K_{\text{PT2}} \cdot (\omega_0)^2}{s^2 + 2 \cdot D \cdot \omega_0 \cdot s + (\omega_0)^2} \tag{1}$$

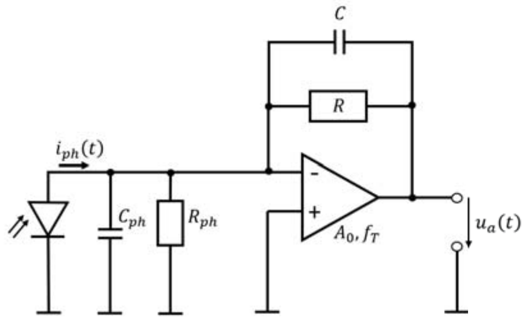

Fig. 3 Transimpedance amplifier as a 2nd order system

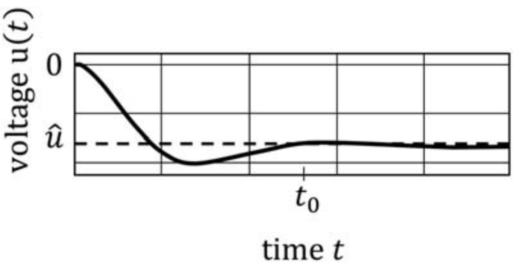

Fig. 4 Step response of TIA: 2nd order system

B. State Space Model & Stability of the TIA

From the listed literature, the state space representation of the systems is used on the one hand for system analysis and on the other hand for multidimensional controller design [3], [4], [7], [8]. The system analysis plays an important role in this elaboration, especially with regard to the main sections of this paper. The transfer to the state space also results in a completely new state and system assessment possibility, it is the phase space. In the state space, states are defined and derived. The phase space uses these derived states and relates them to each other. For example, an arbitrary state x_i and its velocity $\dot{x}_i$ can then be plotted and considered in the phase plane.

In this section, the equations of the TIA are transformed into the state space as an example in order to be able to transform the mathematical description of the photodiode amplifier as well using the same methodology:

$$\dot{\boldsymbol{x}} = \boldsymbol{A} \cdot \boldsymbol{x} + \boldsymbol{B} \cdot \boldsymbol{u} \tag{2}$$

$$y = \boldsymbol{C} \cdot \boldsymbol{x} + \boldsymbol{D} \cdot \boldsymbol{u} \tag{3}$$

Since this is a single input single output system, the u vector becomes a scalar $\boldsymbol{u} \rightarrow u$, the input matrix an input vector $\boldsymbol{B} \rightarrow \boldsymbol{b}$, followed by an output vector $\boldsymbol{C} \rightarrow \boldsymbol{c}^T$ and a direct pass-through value $\boldsymbol{D} \rightarrow d$. However, since there is no direct pass-through at all (input has no directly additive influence on output), it follows that $d = 0$ and the eigenvalues λ_i can be calculated [3], [4].

$$\boldsymbol{A} = \begin{bmatrix} 0 & 1 \\ -(\omega_0)^2 & -2D\omega_0 \end{bmatrix} \tag{4}$$

The system matrix $\boldsymbol{A}$ carries the intrinsic dynamics information in the sense of eigenvalues λ_i.

$$\boldsymbol{b} = \begin{bmatrix} 0 \\ K_P \cdot (\omega_0)^2 \end{bmatrix} \tag{5}$$

The input vector $\boldsymbol{b}$ carries the extrinsic dynamics information of the system, which is caused by external influence.

$$\boldsymbol{c}^T = \begin{bmatrix} 0 & 1 \end{bmatrix} \tag{6}$$

The output vector $\boldsymbol{c}^{\mathrm{T}}$ describes what influence the states x_i of a system have on its output $y = u_{\mathrm{a}}$.

As already mentioned, the eigenvalues of the system can now be determined by the system matrix and the following equation:

$$\det(\lambda \cdot \boldsymbol{I} - \boldsymbol{A}) = 0 \tag{7}$$

$$\left| \begin{bmatrix} \lambda & -1 \\ (\omega_0)^2 & (\lambda + 2D\omega_0) \end{bmatrix} \right| = 0$$

$$\lambda^2 + 2D\omega_0 \cdot \lambda + (\omega_0)^2 = 0$$

$$\Rightarrow \lambda_{1,2} = -D\omega_0 \pm \sqrt{(D\omega_0)^2 - (\omega_0)^2} \tag{8}$$

III. Photodiode Amplifier

The transmission behavior of the initially simulated amplifier circuit is to be determined and can serve as a basis for a later control [3]. Here, the results are collected of the the circuit version intended for practical tests. The electrical circuit used in this elaboration is a modified version of a photodiode amplifier (PDA), which is based on the TIA [3], [4]. The modified PDA combines and replaces the usually switched multiple filters and the signal pickup of the photodiode current ($i_{\mathrm{ph}}(t)$) and the new draft serves to weigh up the advantages and disadvantages compared to other designs in order to optimise the MIMOS II for planetary measurement. The TIA is extended in such a way that the resulting circuit of the PDA can be divided into three sections. This paper will deal exclusively with the first section described by $h_1(t)$. The other sections are the subject of other papers.

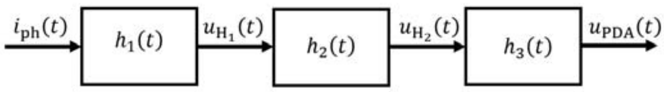

Fig. 5 Photodiode amplifier as a modular system

To describe the first section $h_1(t)$ the Laplace transformation is performed and the transfer function results:

$$\mathcal{L}\{h_1(t)\} = H_1(s) = \frac{U_{H_1}(s)}{I_{ph}(s)} = \frac{b_1 \cdot s + b_0}{s^2 + a_1 \cdot s + a_0} \tag{9}$$

It is a PDT2 element: Proportional differential element, which is doubly delayed.

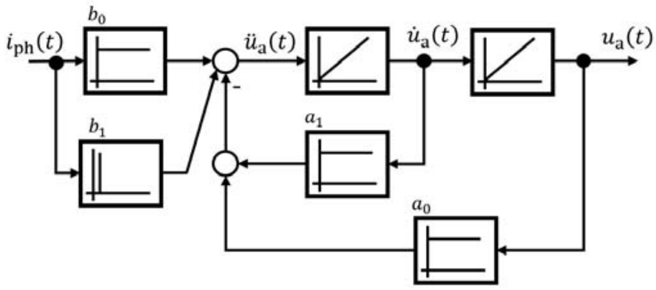

Fig. 6 Block diagram of $H_1(s)$

A. 1st Section of the PDA in the State Space

In this section, the transformation into the state space takes place. For practical reasons, the control normal form (CNF) is used. The CNF makes it possible to write any PTn or PDTn form of the system descriptions directly into a form suitable for the control design and bypasses the controllability analysis, since a control normal form can only be achieved if an original system exists, which can be transformed into the control normal form.

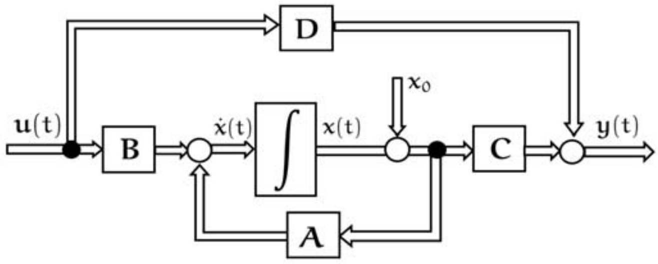

Fig. 7 State space model

$$G(s) = \frac{b_1 \cdot s + b_0}{s^n + a_{n-1} \cdot s^{n-1} + \ldots + a_1 \cdot s + a_0} \tag{10}$$

$$\dot{\boldsymbol{x}}_R = \boldsymbol{A}_R \cdot \boldsymbol{x}_R + \boldsymbol{b}_R \cdot u \tag{11}$$

$$y = \boldsymbol{c}_R^T \cdot \boldsymbol{x}_R + d_R \cdot u \tag{12}$$

$$\boldsymbol{A}_R = \begin{bmatrix} \boldsymbol{0}_{(n-1)} & \boldsymbol{I} \\ & \boldsymbol{a}^T \end{bmatrix} \tag{13}$$

$$\boldsymbol{b}_R = \begin{bmatrix} \boldsymbol{0}_{(n-1)} \\ 1 \end{bmatrix} \tag{14}$$

$$\boldsymbol{c}_R^T = \begin{bmatrix} \boldsymbol{\beta}^{\mathrm{T}} - \boldsymbol{a}^{\mathrm{T}} \cdot b_n \end{bmatrix} \tag{15}$$

$$d_R = d \tag{16}$$

$\boldsymbol{a}^T = \begin{bmatrix} a_0 & a_1 & \ldots & a_{n-1} \end{bmatrix}$ is the vector of the coefficients of the denominator and $\boldsymbol{\beta}^T = \begin{bmatrix} b_0 & b_1 & \ldots & b_{n-1} \end{bmatrix}$ is the vector of the coefficients of the numerator of $G(s)$.

$$\dot{\boldsymbol{x}}_{\mathrm{R}} = \boldsymbol{A}_{\mathrm{R}} \cdot \boldsymbol{x}_{\mathrm{R}} + \boldsymbol{b}_{\mathrm{R}} \cdot u \tag{17}$$

$$y_{\mathrm{R}} = \boldsymbol{c}_{\mathrm{R}}^T \cdot \boldsymbol{x}_{\mathrm{R}} + d_{\mathrm{R}} \cdot u \tag{18}$$

$$\boldsymbol{A}_{\mathrm{R}} = \begin{bmatrix} 0 & 1 \\ -a_0 & -a_1 \end{bmatrix} \tag{19}$$

$$\boldsymbol{b}_{\mathrm{R}} = \begin{bmatrix} 0 \\ 1 \end{bmatrix} \tag{20}$$

$$\boldsymbol{c}_{\mathrm{R}}^T = \begin{bmatrix} b_0 & b_1 \end{bmatrix} \tag{21}$$

$$d_{\mathrm{R}} = 0 \tag{22}$$

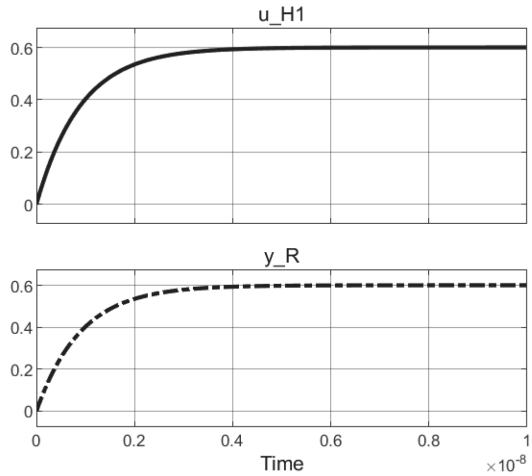

Fig. 8 Step responses of $u_{H_1}(t)$ and state space model y_{R}

A look at the step response of both representations of the system (Fig. 6) clearly shows that they are one and the same system and that each representation has its own justification. The state space opens up a wealth of new possibilities for analysis. For example, stability can be examined on the one hand by means of the poles and on the other hand by means of a visualization in the form of a phase diagram.

Since the classical eigenvalue analysis for the stability assessment of a system presupposes linearity of this system, this method is not applicable in the case of existing nonlinearities. For this reason, the consideration of phase space is relevant and very useful in terms of applicability in all cases.

IV. Stability Analysis of the 1st Section of the PDA

A. Stability of the 1st Section of the PDA in the Laplace Plane

From [4] and [7] the classical stability analysis in state space should be known. The eigenvalues of the system matrix $\boldsymbol{A}_{\mathrm{R}}$ are determined:

$$\det\left(\lambda \cdot \boldsymbol{I} - \boldsymbol{A}_{\mathrm{R}}\right) = 0 \tag{23}$$

$$\left|\begin{bmatrix} \lambda & -1 \\ a_0 & (\lambda + a_1) \end{bmatrix}\right| = \lambda^2 + a_1 \cdot \lambda + a_0 = 0$$

$$\Rightarrow \lambda_{1,2} = -\frac{a_1}{2} \pm \sqrt{\left(\frac{a_1}{2}\right)^2 - a_0} \tag{24}$$

Since in all cases considered and developed in this paper, the system is stable if $\mathrm{Re}\{\lambda_i\} < 0$.

B. Stability of the 1st Section of the PDA in the Phase Plane

Now the stability of the system in the phase diagram is to be considered. For this purpose, the Lyapunov stability is introduced in the first step, which is visualised by the representation in the phase plane.

1) Lyapunov Stability: The stability analysis of nonlinear systems is usually carried out with the direct or second method of Lyapunov. A Lyapunov function $V(\boldsymbol{x})$ is searched which fulfils the following criteria [9, chapt. 4.5], [10, p. 222-236]:

$$\dot{\boldsymbol{x}} = \boldsymbol{f}(\boldsymbol{x}) \tag{25}$$

A real-valued differentiable function $V(\boldsymbol{x})$ is called a Lyapunov function (for the vector field $\boldsymbol{f}$) if $\dot{V}(\boldsymbol{x}) \leq 0$ holds for all points $\boldsymbol{x}$ from the phase space.

$$\dot{V}(\boldsymbol{x}) := \langle \text{grad } V(\boldsymbol{x}), \dot{\boldsymbol{x}} \rangle = \langle \text{grad } V(\boldsymbol{x}), \boldsymbol{f}(\boldsymbol{x}) \rangle \tag{26}$$

$$\dot{\boldsymbol{x}} = \dot{\boldsymbol{x}}(\boldsymbol{x}_{\mathrm{eq}}) = \boldsymbol{0} \tag{27}$$

1) First criterion
   (i) $\boldsymbol{x}_{\mathrm{eq}}$ is an equilibrium of the system
   (ii) V is a Lyapunov function at $\boldsymbol{f}(\boldsymbol{x}_{\mathrm{eq}})$
   (iii) V has a strict local minimum at $\boldsymbol{x}_{\mathrm{eq}}$

2) Second criterion:
   For $\boldsymbol{x} \neq \boldsymbol{x}_{\mathrm{eq}}$ in an environment of the equilibrium $\boldsymbol{x}_{\mathrm{eq}}$, $\dot{V}(\boldsymbol{x}) < 0$ is valid.

It is noticeable that the mathematical description of a Lyapunov function is time-consuming. Especially since no criterion is presented that estimates in advance whether a Lyapunov function exists for a given system of differential equations. In the linear case, a prediction regarding the existence of V can be given quickly and reliably through the eigenvalue analysis. In the nonlinear case, however, no clear structure for estimating the existence of Lyapunov functions is known. The representation of a system in the phase space is intended to provide a possible structure for estimation at this point.

2) Extended Lyapunov Stability in the Phase Plane: The following relationship is already known from the state space description of the system $H_1(s)$:

$$x_1 = u_{H_1} \tag{28}$$

$$x_2 = \dot{x}_1 \tag{29}$$

Now the system is plotted in the phase diagram (Fig. 9). For this purpose, the states are set in relation to each other. The following is to apply:

$$x_1 = f(x_2) \tag{30}$$

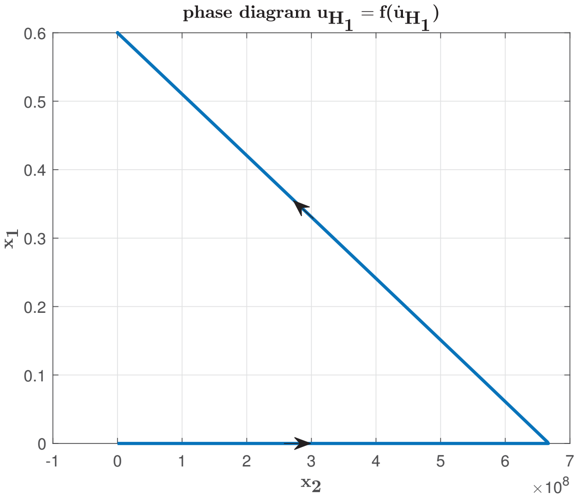

Fig. 9 Phase diagram of the step response of the 1st section of the PDA

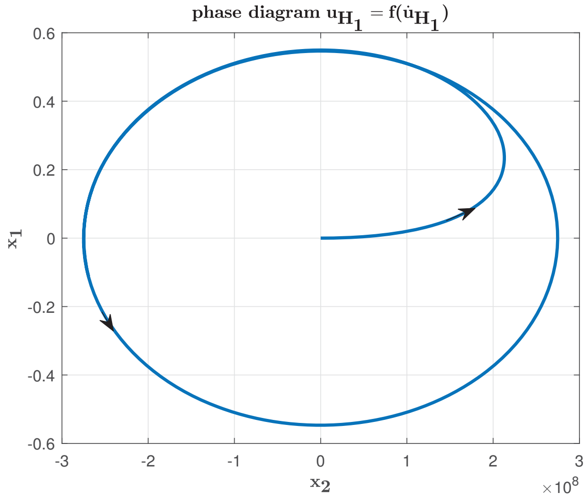

Fig. 10 Phase diagram of the vibration response of the 1st section of the PDA

The phase diagram shows a completely new and different representation of the system. This circumstance is also imperative, since, mostly due to the non-linearities, no regular examination of the system can take place. At first glance, the representation in the phase diagram is hardly meaningful. Even with experience, an accurate statement regarding the stability of the system cannot always be made. For this reason, the solution for a better estimation of the existence of a Lyapunov function lies in the analytical approach of the investigation in phase space. In other words, a systematic approach must be created that will produce a statement regarding the system.

The solution lies in the excitation of the system. In the case of a step-like excitation, the response must already be known in order to classify the system correctly. With an oscillating excitation, the expected response is an oscillation. In phase space, an oscillation is represented as a closed circular or elliptical curve in case that the system is stable. Ideally, a closed circle is expected as in Lissajou's figures in electrical engineering. For this reason, the input function $i_{\text{ph}}(t)$ is set to the following function:

$$i_{\text{ph}}(t) = i_0 \cdot \sin(\omega_x \cdot t) \cdot \sigma(t) \tag{31}$$

$$\sigma(t) = \begin{cases} 0, & t < 0 \\ 1, & t \geq 0 \end{cases} \tag{32}$$

The amplitude is usually set to the value $i_0 = 1$, but the frequency ω_x can be adjusted according to the system. In the standard case, the frequency ω_x should not be set to the resonance frequency ω_0 of the system in order to avoid excessive resonance. In addition, the set frequency ω_x must not coincide with the zero points of the system, as the zero points would then equalise and the excitation would be virtually swallowed up by the system. Fig. 10 shows the system response to an excitation with a harmonic oscillation.

The expected response also occurred with the pure vibration excitation – a closed circular elliptical curve. The coordinate origin represents the initial condition in the solution of the differential equations. In Fig. 11, the excitation is initially step-like and also oscillating-like to demonstrate the transition of these two system responses.

$$i_{\text{ph}}(t) = i_0 \cdot \sigma(t) + i_0 \cdot \sin(\omega_x \cdot t) \cdot \sigma(t) \tag{33}$$

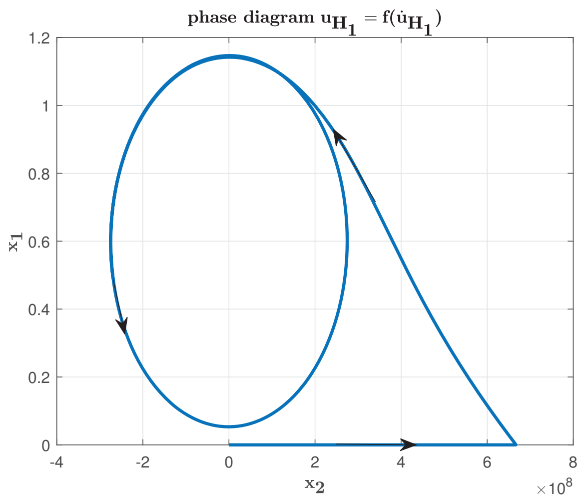

Fig. 11 Phase diagram of step & vibration response of the 1st section of the PDA

It can be clearly seen that the original excitation smoothly transitions into a closed elliptical curve. So it is clear that the system must be stable to allow such a transition. Due to the closed curve, an exact calculation of the Lyapunov function is no longer necessary. Of course, such a function can be determined, but in this case the area to be examined is so clearly delineated that stability can already be confirmed visually.

Now follows the consideration of an unstable system with the described procedure for analysis. The poles of the previous system are shifted to the right half-plane, so there is definitely instability. Then the excitation takes place with an oscillation.

It is to be expected that there will be no closed curve. Fig. 12 shows this investigation.

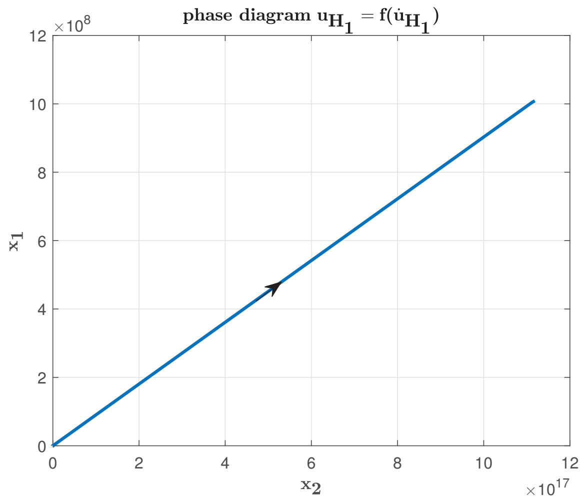

Fig. 12 Phase diagram of the vibration response of the unstable PDA

There is no longer a closed curve. It is a rising straight line in phase space. Thus, a clear statement can be made as to whether a Lyapunov function exists. There is no area in the phase plane that offers indications of stability.

Lyapunov's extended method can thus unambiguously define good approaches for stability ranges and allows good estimates without further calculations up to the unambiguous proof of stability in the linear case.

V. Controller Design for the 1st Section of the PDA

The state regulator can be determined much more simply from the CNF using the following rule:

$$\boldsymbol{k}_R^T = \boldsymbol{\alpha}^T - \boldsymbol{a}^T \tag{34}$$

where $\boldsymbol{\alpha}^T = \begin{bmatrix}\alpha_0 & \alpha_1 & \dots & \alpha_{n-1}\end{bmatrix}$ is the vector of the new coefficients resulting from the pole specification of the form:

$$(s-s_{p1,\alpha})\cdot(s-s_{p2,\alpha})\cdot\ldots\cdot(s-s_{pn,\alpha}) = s^n+\alpha_{n-1}\cdot s^{n-1}+\ldots+\alpha_1\cdot s+\alpha_0$$

$$v = \left[\boldsymbol{c}^T(\boldsymbol{b}\boldsymbol{k}^T - \boldsymbol{A})^{-1}\boldsymbol{b}\right]^{-1} \tag{35}$$

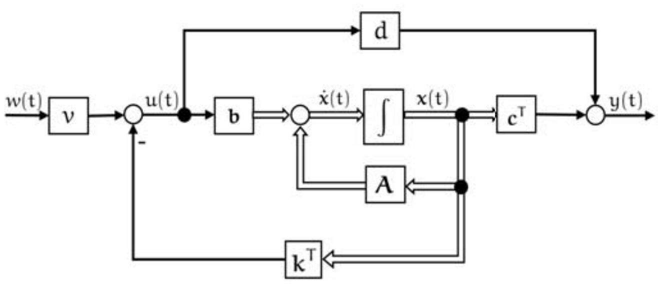

Fig. 13 Controller and prefilter in the state space

The new coefficients were based on the old ones:

$$\boldsymbol{\alpha}^{\mathrm{T}} = 5\cdot\boldsymbol{a}^{\mathrm{T}} = 5\cdot\begin{bmatrix}a_0 & a_1\end{bmatrix} \tag{36}$$

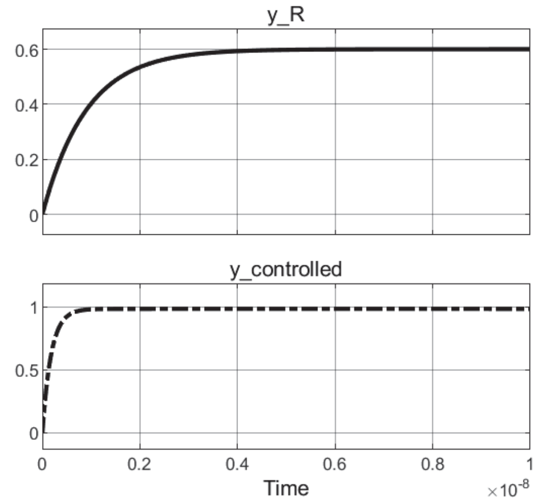

Fig. 14 Controlled system

The controlled system has a very fast response behaviour. The factor 5 is an experimental value from the laboratory and can vary depending on the realisation possibilities of the system.

VI. Conclusion

A. Linear System Analysis

System analysis in the linear case has been known and well defined for a long time. Eigenvalue analysis provides a very good method of investigation at this point [7]. However, for higher order systems, the time required to find analytical solutions can increase enormously. Numerical methods for the approximate solution of eigenvalue problems provide a remedy. On the other hand, the extended Lyapunov method for pure visualisation in phase space can save an enormous amount of time.

B. Nonlinear Stability Analysis

Stability analysis for non-linear systems is much more challenging than for linear systems. The time required for the determination of analytical solutions and the derivation of a possible Lyapunov function is relatively high. Even with systems that are not too complex, it is hardly possible to make a statement regarding the existence of a Lyapunov function [9], [10]. The extended Lyapunov method for pure visualisation in phase space enables a very good first estimation and delimitation of areas in which a Lyapunov function can exist. This saves time and resources, both in theoretical and applied research.

C. Analysis of $H_1(s)$ of the PDA

The transfer of $H_1(s)$ (9) into the state space, in particular into the control normal form, enables a multidimensional analysis and leads to a consideration on several levels. The control normal form presupposes controllability, since a basis system matrix $\boldsymbol{A}$ must always exist in advance of this normal form so that a transformation into $\boldsymbol{A}_{\mathrm{R}}$ can take place [7].

With regard to the stability of the first section of the PDA, a stable system could be demonstrated in two ways. Both the eigenvalue analysis and the extended direct method according to Lyapunov, presented in this paper, have produced clear results.

D. Controller Design and Its Challenges

The controller design essentially depends on the nature of the possible circuit parameters in the real design. This means that it is one thing to design the controller simulatively, but quite another to implement the real controller. In the real version, resistors and capacitors were used and care must always be taken to ensure that the component noise does not predominate with these fine settings and distort the poles of the system and thus negatively influence and shift them. However, the results obtained here are satisfactory and open up a further view in the direction of very fine controller designs.

VII. Outlook

With the development of the new light processing system, measurements can be made in less time and with higher resolution. Based on the results from this paper, the following points should be addressed and elaborated in future papers:

- The other two sections ($h_2(t)$, $h_3(t)$) of the overall system $h(t)$ should also be examined in order to satisfy the following form for the overall description:

$$\mathcal{L}(h(t)) = H(s) = H_1(s) \cdot H_2(s) \cdot H_3(s) \tag{37}$$

- A state estimation is essential for more precise controller settings and should be taken into account in future work.
- Following this, the overall system can then be analyzed.

Acknowledgments

The authors would like to thank the UMB-II project, the German Aerospace Center (DLR), Hannover School for Nanotechnology (hsn), Leibniz University Hannover (LUH), Laboratory of Nanotechnology and Quantum Engineering (LNQE) and Hochschule Hannover – University of Applied Sciences and Arts (HsH).

References

[1] M. Blumers, B. Bernhardt, P. Lechner, G. Klingelhöfer, C. dUston, H. Soltau, L. Strüder, R. Eckerhardt, J. Brückner, H. Henkel, J.G. Lopez, J. Maul, 'The miniaturised Mössbauer spectrometer MIMOS II A: Increased sensitivity and new capability for element alanalysis', Nuclear Instruments and Methods in Physics Research A 624 (2010) 277281. journalhomepage: www.elsevier.com/locate/nima, 2010

[2] G. Klingelhöfer, B. Fegley, R.V. Morris, E. Kankeleit, P. Held, E. Evlanov, O. Priloutskii, Planetary and Space Science, 44, 11, 1277-1288 (1996).

[3] M. Beyki, J. Pawlak, R. Patzke, F. Renz,'Simulation of the electronic part of Mössbauer spectroscopy', OHJG 2023, Okayama, Japan, DOI: https://doi.org/10.25968/opus-2459 .

[4] M. Beyki, J. Pawlak, R. Patzke, F. Renz,'Simulative Development of the Electronic Component of Mössbauer Spectroscopy with a Focus on the Controllability of a 2nd Order Transimpedance Amplifier', Lux Junior 2023, Ilmenau, Germany, DOI: 10.22032/dbt.55787, https://www.tu-ilmenau.de/fileadmin/Bereiche/MB/lichttechnik/Lux_junior/2023/Beyki_Lux_junior_2023.pdf

[5] X. Ramus, 'Transimpedance Considerations for High-Speed Amplifiers', Texas Instruments: Application Report SBOA122 November 2009, https://www.ti.com/lit/an/sboa122/sboa122.pdf.

[6] R. Patzke, 'Schnelle und rauscharme Photonenmessung mit pin-Fotodioden', Hochschule Hannover – University of Applied Sciences and Arts, Fachgebiet Integrierte Schaltungen und Eingebettete Systeme (IES),
DOI: https://doi.org/10.25968/opus-2315, 31/July/2022.

[7] O. Föllinger, U. Konigorski, B. Lohmann, G. Roppenecker, A. Trächtler, 'Regelungstechnik: Einführung in die Methoden und ihre Anwendung', 13th edition, *VDE VERLAG GMBH* 2022, p. 168 - 188.

[8] M. Beyki, R. Kutzner, U. Lindemann, 'Systemtheorie & Optimale Regelung – Teil V Zustandsregelung', 1st edition, Hochschule Hannover – University of Applied Sciences and Arts,
DOI: https://doi.org/10.25968/opus-2442 .

[9] J. Adamy, 'Systemdynamik und Regelungstechnik II – Teil II: Nichtlineare Systeme', Shaker Verlag, Aachen, 2005, chapt. 4.5.

[10] H. Unbehauen, 'Regelungstechnik II – Zustandsregelungen, digitale und nichtlineare Regelsysteme', 9th edition, Vieweg Verlag, Wiesbaden, 2007, p. 222-236.